

# A self-assembled leucine polymer sensitizes leukemic stem cells to chemotherapy by inhibiting autophagy in acute myeloid leukemia

Xi Xu,<sup>1,2\*</sup> Jian Wang,<sup>3\*</sup> Tong Tong,<sup>4\*</sup> Wenwen Zhang,<sup>2</sup> Jin Wang,<sup>2</sup> Weiwei Ma,<sup>5</sup> Shunqing Wang,<sup>5</sup> Dunhua Zhou,<sup>3</sup> Jun Wu,<sup>1,4</sup> Linjia Jiang<sup>1</sup> and Meng Zhao<sup>2</sup>

<sup>1</sup>Guangdong Provincial Key Laboratory of Malignant Tumor Epigenetics and Gene Regulation, Sun Yat-sen Memorial Hospital, Sun Yat-sen University; <sup>2</sup>Key Laboratory of Stem Cells and Tissue Engineering (Ministry of Education), Zhongshan School of Medicine, Sun Yat-sen University; <sup>3</sup>Department of Pediatrics, Sun Yat-sen Memorial Hospital, Sun Yat-sen University; <sup>4</sup>Key Laboratory of Sensing Technology and Biomedical Instrument of Guangdong Province, School of Biomedical Engineering, Sun Yat-sen University and <sup>5</sup>Department of Hematology, Guangzhou First People's Hospital, School of Medicine, South China University of Technology, Guangzhou, Guangdong, China.

\*XX, JW and TT contributed equally as co-first authors.

**Correspondence:** M. Zhao  
[zhaom38@mail.sysu.edu.cn](mailto:zhaom38@mail.sysu.edu.cn)

L. Jiang  
[jianglj7@mail.sysu.edu.cn](mailto:jianglj7@mail.sysu.edu.cn)

J. Wu  
[wujun29@mail.sysu.edu.cn](mailto:wujun29@mail.sysu.edu.cn)

**Received:** November 4, 2021.

**Accepted:** March 10, 2022.

**Prepublished:** March 17, 2022.

<https://doi.org/10.3324/haematol.2021.280290>

©2022 Ferrata Storti Foundation

Published under a CC BY-NC license



## **Supplementary information**

### **Patient specimens**

The AML patients' specimens were derived from the routine clinical management in the Sun Yat-sen Memorial Hospital. The sample use was approved by the ethics committee at Sun Yat-sen Memorial Hospital in accordance with international guidelines and the ethical standards outlined in the Declaration of Helsinki. Mononuclear cells were isolated from BM by standard Ficoll-Hypaque gradient density centrifugation, then processed to extract protein for Western blots.

### **TARGET database analyses.**

Data were obtained from the TARGET (Therapeutically Applicable Research To Generate Effective Treatments) database, AML (Acute Myeloid Leukemia) project (<https://ocg.cancer.gov/programs/target>; accessed August 24<sup>th</sup>, 2020). Patient samples were separated into two groups based on high (n = 147 samples) or low (n = 148 samples) expressions of ATG5 or ATG7.

### **Single-cell RNA-seq and data analysis**

We started the treatment 28 days after transplantation when the chimeric rate of leukemia cells (GFP<sup>+</sup>) reached about 80% in the peripheral blood of AML mice. The cells from the femoral and tibial BM of the lower limbs of AML mice that had undergone fissure on the second day after chemotherapy or PBS treatment. Cell viability (>75%), cell labeling, RNA bank building, and sequencing were carried out according to the experimental procedure. After the sequencing results were analyzed, cells with less than 300 genes and genes expressing less than three cells were excluded. The remaining cells underwent dimensionality reduction and grouping by t-distributed stochastic neighbor embedding (t-SNE). Cells that do not express the MLL-AF9 gene were defined as normal cells. The Wilcoxon Rank-Sum Test was used to detect differential genes between different groups, Gene Set Enrichment Analysis (GSEA), with MSigDB gene sets, were used to identify pathways having induced or repressed expression in each cell group by revised GSEA\_R v1.2 R package ([https://github.com/GSEA-MSigDB/GSEA\\_R](https://github.com/GSEA-MSigDB/GSEA_R)) with default parameters.

### **Western blots**

The equivalent number of cells ( $1 \times 10^6$ ) were sorted into PBS with 2% FBS. Then, the

cells were washed with PBS and lysed by RIPA. Protein extracts from an equal number of cells ( $5 \times 10^5$  per sample) were fractionated by 10% SDS-PAGE and transferred to a PVDF membrane (IPVH00010, Merck Millipore). After being blocked with 5% non-fat milk in Tris-buffered saline with Tween-20 (TBST, pH 7.6) for 1 h at room temperature, the membranes were incubated with primary antibodies: anti-LC3B I/II (mouse, 1:1000, 83506S, Cell Signaling Technology), anti-p-mTOR (Ser2448, rabbit, 1:1000, 5536T, Cell Signaling Technology), anti-p-S6 (Ser235/256, rabbit, 1:1000, 4858T, Cell Signaling Technology), anti-p-4EBP1 (Ser65, rabbit, 1:1000, 13443S, Cell Signaling Technology), or anti- $\beta$ -actin (rabbit, 1:1000, 4970, Cell Signaling Technology) overnight at 4 °C and then incubated with secondary antibodies (rabbit, 1:10,000, W401B, Promega; mouse, 1:10,000, W402B, Promega) for 1 h at room temperature. The blots were detected by X-ray film or digital imaging system (Odyssey Fc). Protein levels were quantified with densitometric intensity.

### **Preparation and characterization of Leu-DOX and DOX@PLGA**

Leu-DOX and DOX@PLGA were prepared by the nanoprecipitation method. Briefly, DOX, with 8L6 or PLGA (805149, Sigma-Aldrich) polymer, and DSPE-mPEG<sub>2000</sub> were dissolved and mixed in dimethyl sulfoxide with a certain volume ratio. Then the mixture was added dropwise slowly into ultrapure water under constant stirring. The size distribution and zeta-potential of Leu-DOX were further measured by dynamic light scattering (DLS, Malvern Zetasizer Nano-ZS90).

### **Drug release experiment**

Leu-DOX was sealed in dialysis bags (MWCO:3500 Da). Then the dialysis bags were placed in different pH environments, which were created by the different volume ratios of citric acid and sodium hydrogen phosphate solutions. The system was put in a constant temperature shaker (37°C, 100 rpm). After that, at the specific time point, 500  $\mu$ l medium in the buffer solution was taken out, and the equal volume of buffer was added back. The concentrations of DOX were measured through the standard curve method by ultraviolet spectrum ( $\lambda_{\text{abs}}=480$  nm). Then the cumulative release of DOX was calculated at each time point.

### **The particle size and morphology of Leu-DOX**

The Leu-DOX solution was dropped onto the carbon-coated copper net. Particle size and morphology were observed with a transmission electron microscope (manufacturer) after negatively staining with the phosphotungstic acid solution. Before determination, Leu-DOX solution was diluted to  $0.5 \text{ mg ml}^{-1}$ ,  $90^\circ$  scattering angle,  $25^\circ \text{ C}$  with three independent replicates. The nanoparticles were placed in 1xPBS and RPMI 1640 medium containing 10% FBS for 7 days. The corresponding particle size and Polymer dispersity index (PDI) were recorded every day to determine the long-term stability of the nanoparticles.

### **Stability assay**

Leu-DOX was placed at room temperature for 72 h, and their particle size was measured by Zetasizer Nano ZS90 at the indicated time points for a stability curve.

### **Drug loading and encapsulation rate of Leu-DOX**

Leu-DOX and DOX@PLGA were dispersed in acetonitrile solution. After high-speed centrifugation and filtration, the content was determined by HPLC. The chromatographic conditions were as follows: mobile phase (water: acetonitrile=30:70), flow rate 1 ml per min, UV detection wavelength 230 nm, and the sample volume was  $10 \mu\text{L}$ , and the column temperature was  $25^\circ \text{ C}$ . The drug loading capacity and drug loading efficiency of nanoparticles were calculated:

Drug loading (wt%) = DOX mass in nanoparticles / mass of nanoparticles  $\times 100\%$

Drug loading efficiency (wt%) = DOX mass in nanoparticles / total DOX added amount  $\times 100\%$

### **Cell uptake assay**

THP-1 cells were inoculated in a 15 mm glass-bottomed cell culture dish, cultured at  $37^\circ \text{ C}$  for 24 h, then treated with DOX, Leu-DOX, or DOX@PLGA for 0, 2, 4, or 8 h. The collected cells were stained by Dapi (1306, Thermo Scientific), fixed with 4% PFA for 15 minutes, and DOX fluorescence intensity was observed through a high-speed confocal imaging system (Dragonfly CR-DFLY-202 2540).

### **Flow Cytometry**

Peripheral blood ( $20\text{-}30 \mu\text{L}$ ) were taken through the tail vein of mice and added to the anticoagulation tube. BM cells were taken from the femur and tibia of the sacrificed

mice. The red blood cells were lysed, and the BM cells and peripheral blood cells were filtered using a 70  $\mu\text{m}$  cell strainer. The anti-Mac-1 (M1/70, Biolegend) and anti-c-Kit (2B8, Biolegend) (all used as 50 ng per million cells) antibodies were used for staining. 7-aminoactinomycin D (7-AAD, A1310, Life technologies) was used to exclude dead cells. In the DiL@8L6 uptake experiment, the MLL-AF9 derived mice were injected with DiL (22102, ATT Bioquest), or DiL@8L6 through the tail vein at  $0.3 \text{ mg kg}^{-1}$  when the proportion of GFP<sup>+</sup> cells in the peripheral blood reaches 20%. BM cells from the femur and tibia were collected 48 h after injection. Monoclonal antibodies, anti-CD3 (145-211, Biolegend), anti-CD4 (GK1.5, ebioscience), anti-CD8 (53-6.7, ebioscience), anti-B220 (RA3-6B2, Biolegend), anti-IFN $\gamma$  (XMG1.2, ebioscience), anti-Mac1, anti-Gr1 (RB6-8C5, ebioscience), anti-Ter-119 (RER-119, Biolegend), anti-IgM (Eb121-15F9, ebioscience), anti-Sca-1 (D7, ebioscience), anti-c-Kit, anti-Ly6G (RB6-8C5, ebioscience), anti-Ly6C (N418, ebioscience), anti-CD11c (2B8, ebioscience), anti-NK1.1 (PK136, ebioscience), anti-F4/80 (BM8, ebioscience) (all used as 50 ng per million cells) were used for staining. The samples were analyzed and sorted using the Attune NxT flow cytometer (Thermo) or FACS Aria III (BD), and the results were analyzed using Flowjo software.

### ***In vivo* imaging**

The MLL-AF9 derived mouse was taken as an AML leukemia model when the proportion of GFP<sup>+</sup> cells in the peripheral blood reached 70%. AML mice were injected with DiR dye (22070, Ruixibo) or DiR@8L6 through the tail vein at  $0.5 \text{ mg kg}^{-1}$  bodyweight. At the indicated time point, the mice were anesthetized and imaged with the *in vivo* imaging system (PerkinElmer's IVIS Lumina XRMS). Finally, the mice were sacrificed by cervical dislocation, and the heart, lung, spleen, liver, kidney, femur, and tibia were collected for *ex vivo* imaging. Quantification of the fluorescence signal was performed using Living Image Software (IVIS Lumina XRMS, USA).

### **ATG5 knockdown**

ATG5 (human) shRNA (CCTTTCATTCAGAAGCTGTTT) and random control shRNA were cloned into pLKO.1-puro (8453, Addgene). ATG5 knockdown and control lentivirus were prepared by HEK293T transfected by pLKO.1-puro together with psPAX2, pMD2G packaging vectors. THP-1 cells were infected with

ATG5-knockdown or control lentivirus and further selected by  $1 \mu\text{g mL}^{-1}$  puromycin (4089, R&D) for 48 h where indicated.

### **Comet assay**

The alkaline comet assay was performed following instruction of the manufacturer (Trevigen, 4250-050-K).

### **Statistics**

Data are expressed as mean  $\pm$  s.d. Experiments were analyzed by Student's t-test \*  $P < 0.05$ , \*\*  $P < 0.01$ , \*\*\*  $P < 0.001$ ; or Repeated-measures one-way analysis of variance (ANOVA) followed by Dunnett's test for multiple comparisons †  $P < 0.05$ , #  $P < 0.01$ , ##  $P < 0.001$ . as indicated. The survival of the two groups was analyzed using a log-rank test. Differences were considered statistically significant if  $P < 0.05$ .

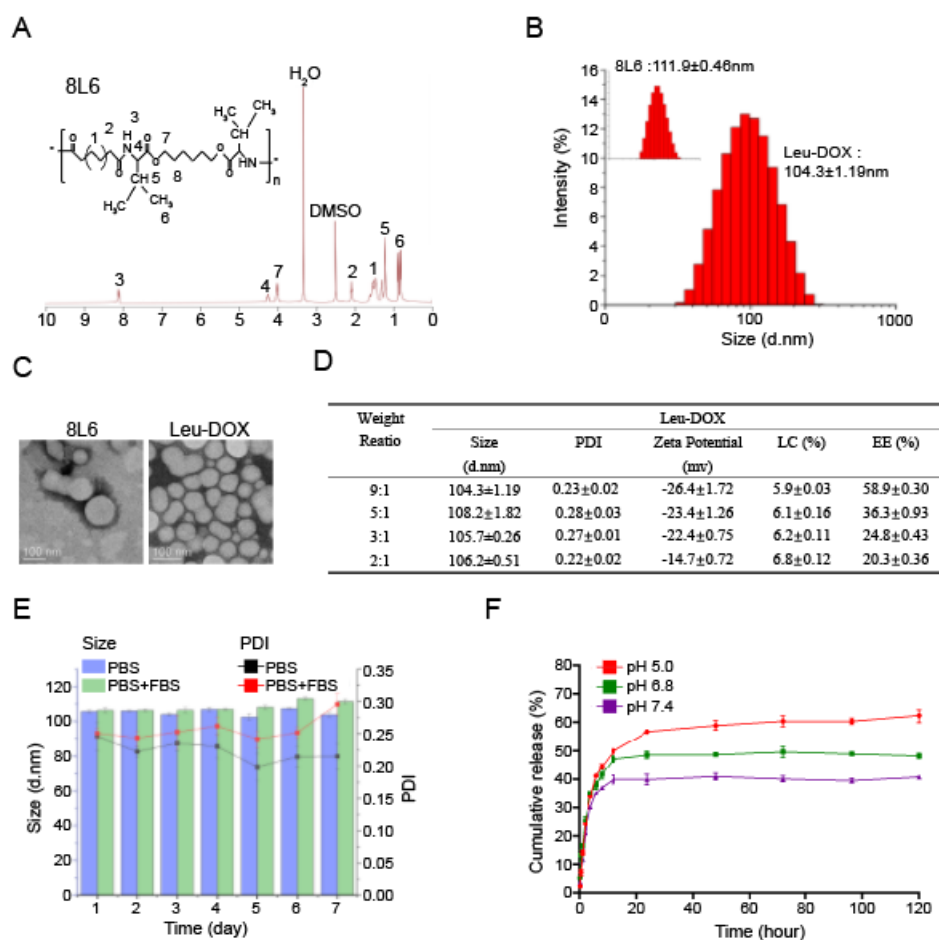


**Figure S1. The characterization of leucine self-assembled drug carrier 8L6 and Leu-DOX.**

(A) Nuclear magnetic resonance graph of 8L6. (B) Particle size distribution of 8L6 and Leu-DOX. (C) TEM image of 8L6 and Leu-DOX. (D) The encapsulation efficiency and drug loading of DOX in Leu-DOX. (E) Stability of Leu-DOX. (F) Drug release behavior of Leu-DOX in different pH solutions.

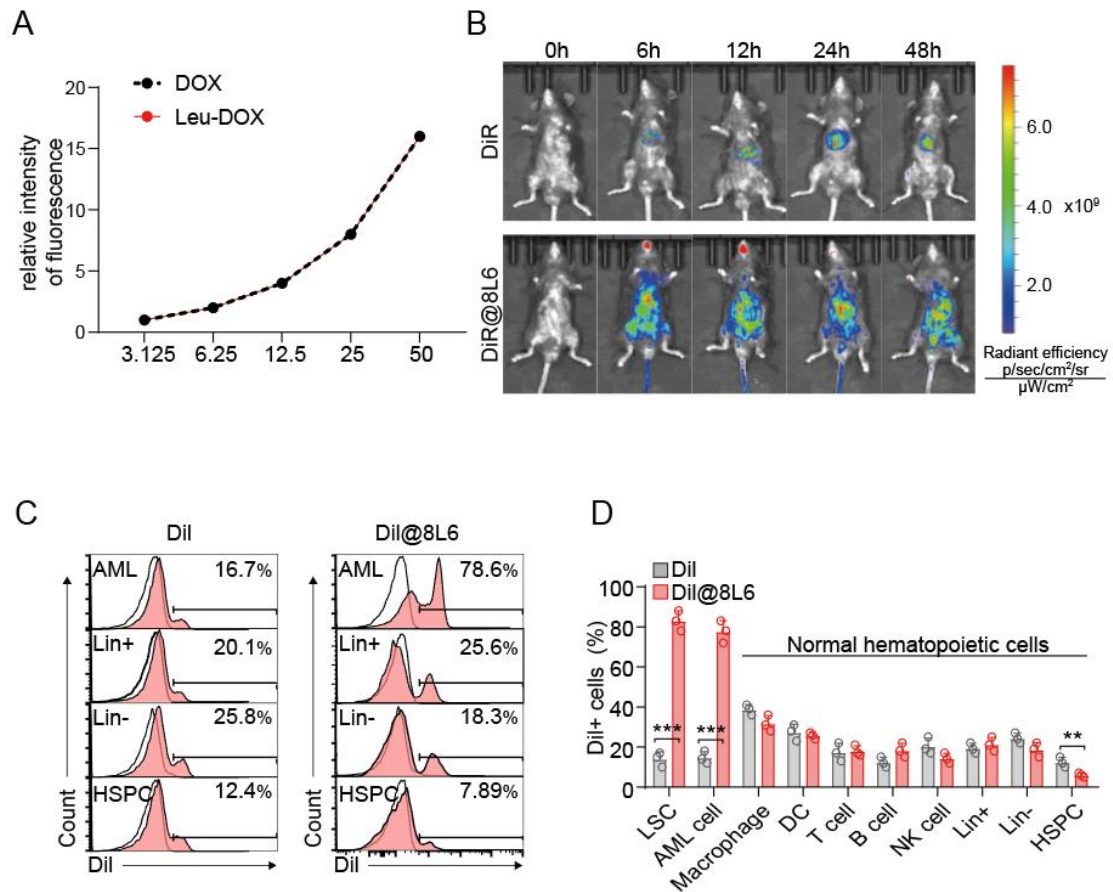


**Figure S2. The fluorescence intensity of DOX and Leu-DOX and distribution of DiI@8L6 in AML mice.**

(A) The fluorescence intensity of DOX and Leu-DOX. The DOX and Leu-DOX were diluted by a gradient and detected by a spectrophotometer. (B) The fluorescence images of DiI in AML mice at the indicated time after DiI or DiI@8L6 injection. (C-D) Representative flow cytometry profile (C) and quantitative (D) of the intensity of DiI fluorescence in different hematopoietic cell populations. DiI fluorescence was quantified 12 h after injection. (n=3 mice per group).

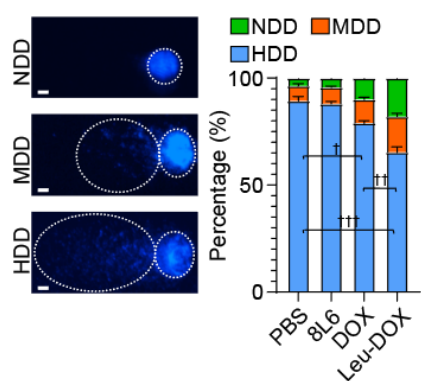


**Figure S3. Leu-DOX induces more DNA damage in AML cells.**

Representative image (left) and quantification (right) of comet assay in THP-1 cells 72 h after indicated treatments (n=30 cells). NonDamaged DNA (NDD), Moderately Damaged DNA (MDD), Heavily Damaged DNA (HDD).

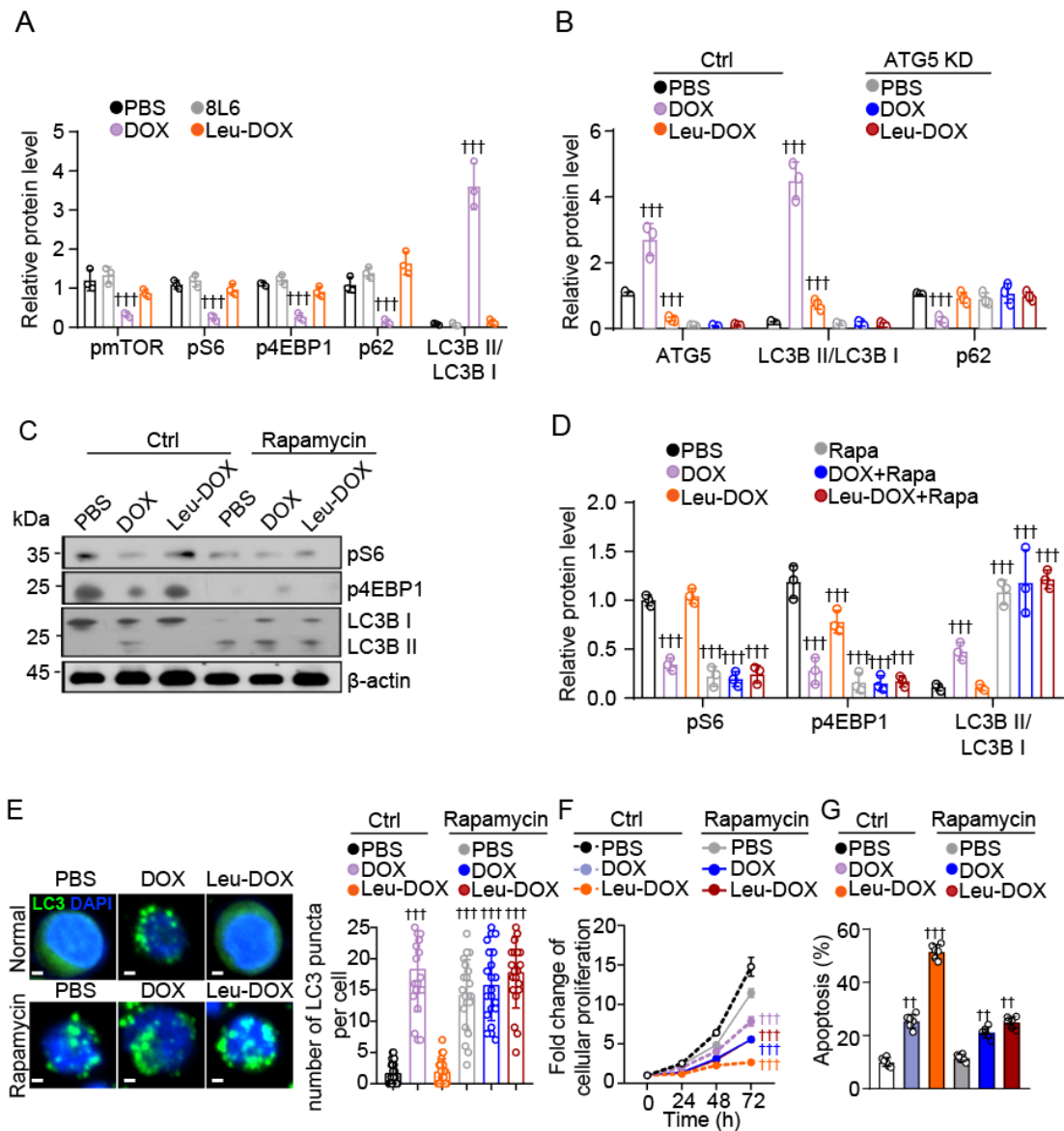


**Figure S4. Leu-DOX inhibits autophagy to enhance chemotherapy efficacy in AML cells.**

(A) Quantification of western blots in Figure 4A. (B) Quantification of western blots in Figure 4C. (C) Western blots of the pS6, p4EBP1, and LC3 in THP-1 cells 48 h after indicated treatment. (D) Quantification of western blots in Figure 4G. Three independent experiments were performed. Protein levels were measured with the densitometric intensity.  $\beta$ -actin was used as a loading control. (E) Representative images (left) and quantification (right) of LC3 puncta in THP-1 cells 48 h after indicated treatment. (Scale bar=3  $\mu$ m). (n=20 cells) (F) The cell proliferation rate of THP-1 cells after indicated treatment. (n=6 replicates) (G) The apoptosis rate of THP-1 cells 72 h after indicated treatment. (n=6 replicates).

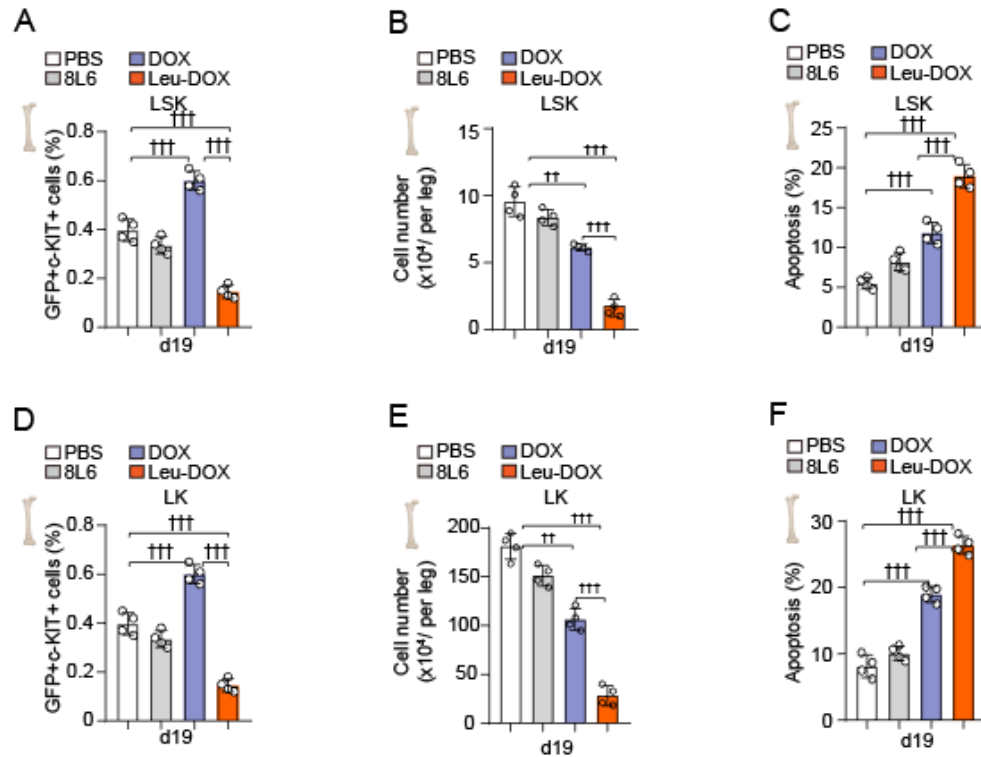


**Figure S5. Leu-DOX reduces LSC enriched cells in AML mice.**

(A-C) the frequency (A), absolute number (B), and the apoptosis rate (C) of GFP<sup>+</sup>Lin<sup>-</sup>Sca1<sup>+</sup>c-KIT<sup>+</sup> cells in the BM of AML mice at d19 with indicated treatments. (D-F) the frequency (D), absolute number (E), and the apoptosis rate (F) of GFP<sup>+</sup>Lin<sup>-</sup>Sca1<sup>-</sup>c-KIT<sup>+</sup> cells in the BM of AML mice at d19 with indicated treatments.

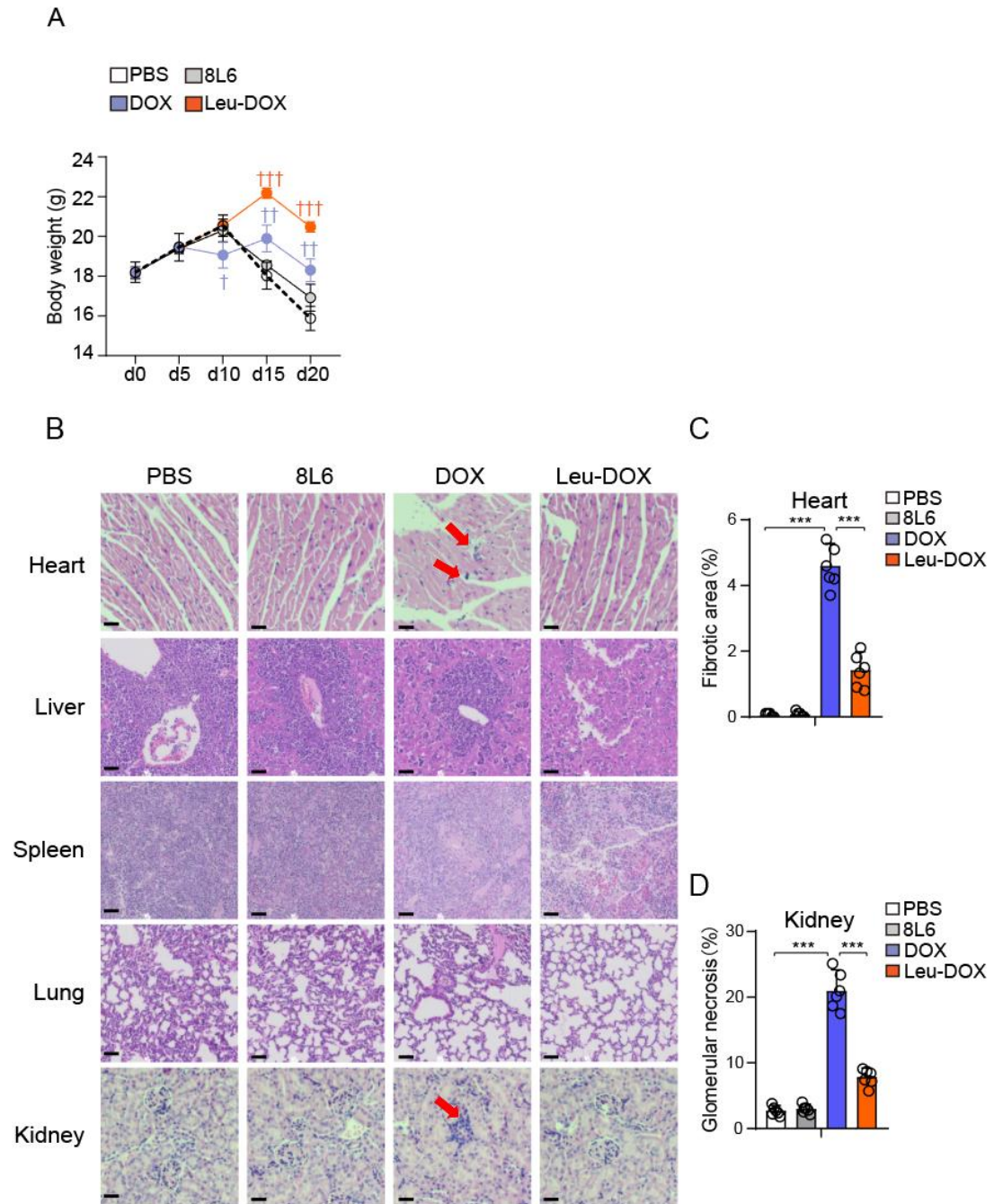


**Figure S6. Leu-DOX treatment has reduced tissue damage in AML mice.**

(A) Bodyweight of AML mice at the indicated time after treatment. (n=5 mice). (B) Major organs stained with hematoxylin and eosin for drug safety evaluation. (Red arrow: Vacuolar degeneration of cardiac cells. Red arrow: Damage of renal cells. (C-D) quantification of heart damage (C), and kidney damage (D) in AML mice at d21 with indicated treatment (Illustrated in Fig. 6A). (Scale bar=100  $\mu$ m).